resistance and thereby preserving the high values of the characteristics of thermoelectric converters under miniaturization conditions, are currently central.

To design thermoelectric modules and calculate their characteristics, the experimentally established contact resistance values are used. As a rule, to measure these values, rather complicated methods and installations are employed [13 – 17]. Contact resistance depends on the technology for producing thermoelectric materials, methods for forming their contacts with metal layers, pre-processing of the surfaces of semiconductor crystals [16, 18 – 20] and other factors. Therefore, the experimental values of contact resistance for specific TEM-metal pairs can differ significantly, which complicates the analysis and optimization of the structure of transient contact layers. Theoretical methods for modeling TEM-metal contacts are practically absent.

Therefore, *the purpose of this work* is to develop a model of the structure of TEM-metal transient contact layers and methods for estimating the electrical contact resistance of such a structure, to calculate the temperature dependences of contact resistance for thermoelements of traditional materials based on BiTe with a view to their further application for the design of thermoelectric power converters, on particular with microminiature legs.

Physical model of TEM-metal transient layer

In thermoelectric modules manufactured by traditional technology, connection of *n*- and *p*-type legs in thermoelements is carried out by interconnect plates made of highly conductive metal, in particular copper. The contact of the semiconductor material with metal interconnects, as a rule, is provided by soldering or connection using a special electrically conductive paste. To restrict the diffusion of interconnect elements and solder or paste into the bulk of a semiconductor leg, a thin anti-diffusion layer of metal, usually nickel, is applied to its surface [21 – 26], which, in addition to low diffusion of elements, provides high adhesion and a reliable electrical contact. After applying the metal to the surface of the thermoelectric material, a transient TEM-metal contact layer arises at the interface. Physical processes in the transient layer are the main cause for contact resistance that occurs when an electric current passes through a thermoelement.

For the effective operation of thermoelectric modules, the contacts must be ohmic [21 – 27]. In ohmic contacts, current carriers pass from semiconductor to metal, overcoming the potential barrier at the TEM – metal interface, which is created due to the difference in the energy band structure of semiconductor and metal [28, 29]. The main characteristic of an ohmic contact is its resistance, reduced to a unit area [30]. This resistance has two main components. The first is the resistance r_l of transient near-contact area, the second – the resistance r_b associated with the transition of charge carriers through the potential barrier at the boundary between the semiconductor and the metal. This second component is commonly called the boundary electrical resistance [31]. However, the purpose of this paper is to calculate the temperature dependences of thermoelectric characteristics of transient layer without taking into account the presence of a potential barrier.

General formulae for thermoelectric characteristics of transient layer

The electrical resistance of transient layer is affected by its composition and structure, which depend on the technology of fabrication of TEM-metal contact. The most common methods of metal deposition on the surface of a semiconductor are the technologies of fusion, sputtering, electroplating, and epitaxy. The structure of transient layer is determined by two basic physical processes. It is mutual diffusion of atoms (molecules) of contacting materials and their chemical interaction [32]. Traditionally, the application of

nickel diffusion layers on the surface of thermoelectric material is carried out by electroplating. As stated in [22,23,32], under the conditions of such technology, the structure of transient layer is characterized by the absence of any chemical compounds of metal atoms with atoms (molecules) of the semiconductor. In this case, the main factor determining the electrical properties of transient layer is considered to be the effect of semiconductor doping with metal due to mutual diffusion [32], which occurs under the conditions of the operating modes of thermoelements. It should be noted that transient layer differs from the bulk thermoelectric material by the inhomogeneous spatial distribution of metal impurity atoms, which leads to the dependence of the electrical conductivity $\sigma_l(x)$ of transient layer on the dimensionless coordinate $x = \tilde{x}/h$ where h is the thickness of transient layer, $x \in [0,1]$. Suppose that electrical conductivity varies continuously from its value σ_m in metal to the value σ_s in thermoelectric material, i.e., function $\sigma_l(x)$ satisfies the requirements.

$$\sigma_m=\sigma_l(0), \quad \sigma_s=\sigma_l(1). \tag{1}$$

To determine the appearance of the dependence $\sigma_l(x)$, we use the concept of the distribution of the volume fraction of an impurity metal in the material of the near-contact transient layer, which is determined by the ratio of the volumes of impurity atoms to all atoms (molecules) of transient layer, which are in the elementary volume of thickness *dx* at a distance *x* from the metal surface *x = 0* and is calculated by the relation

$$v(x) = \frac{\left(A_m/\gamma_m\right)n(x)}{\left(A_m/\gamma_m\right)n(x)+\left(A_s/\gamma_s\right)\left(n_0-n(x)\right)}, \tag{2}$$

where A_s, A_m is the atomic or molecular weight, γ_s, γ_m is the density of semiconductor thermoelectric material and metal, respectively, $n(x)$ is the distribution of the concentration of metal atoms in transient layer, which is established in the steady-state operating modes of the thermoelement due to diffusion, n_0 is the concentration of metal atoms that can diffuse. Formula (2) is correct, subject that part of the elementary volume of transient layer, unoccupied by metal atoms, is considered to be occupied by atoms (molecules) of thermoelectric material.

Function $n(x)$ is a solution of one-dimensional boundary value problem of steady-state diffusion in the presence of a constant source of metal atoms with the boundary conditions $n(0)=n_0$, $n(1)=0$, which under the condition of constancy of diffusion coefficient D and intensity Q of the source with concentration n_0, looks like:

$$n(x) = n_0\left[1-(1-A)x-Ax^2\right]. \tag{3}$$

where n_0 – concentration of atoms in metal, dimensionless parameter $A = Qd_0^2/2Dn_0$ characterizes the mode and conditions of contact creation.

Under these assumptions, the dimensionless function (2) of the distribution of volume fraction of impurity $v(y)$ takes on the form

$$v(y) = \frac{\left(A_m/\gamma_m\right)\left[1-(1-A)y-Ay^2\right]}{\left(A_m/\gamma_m\right)\left[1-(1-A)y-Ay^2\right]+\left(A_s/\gamma_s\right)\left[(1-A)y+Ay^2\right]}, \tag{4}$$

and the following conditions for it are satisfied

$$v(0)=1, \quad v(1)=0. \tag{5}$$

We assume that electrical conductivity proportional to carrier concentration in the case of doping impurity is proportional to concentration of impurity atoms. As a result, the form of coordinate dependence of electrical conductivity of transient layer $\sigma_l(y)$ will be determined by the coordinate dependence (4) of the volume fraction $v(y)$ of metal impurity. Then $\sigma_l(y)$ without regard to percolation effect, when metal atoms do not form clusters, will be determined through $v(y)$ by the function

$$\sigma_l(y) = \sigma_s + (\sigma_m - \sigma_s)v(y), \tag{6}$$

for which, taking into account (5), the requirements of (1) will be satisfied. Formula (6) coincides with classical formula for generalized composite conduction.

With this approximation, the electrical resistance of the near-contact transient layer can be estimated by the formula

$$r_{ce} = h\int_0^1 \frac{dy}{\sigma_l(y)}. \tag{7}$$

The relation similar to (6) is also valid for thermal conductivity of transient layer:

$$\kappa_l(y) = \kappa_s + (\kappa_m - \kappa_s)v(y), \tag{8}$$

where κ_s and κ_m are thermal conductivities of TEM and metal, respectively, so for electrical contact resistance the following relation is valid:

$$r_{ct} = h\int_0^1 \frac{dy}{\kappa_l(y)}. \tag{9}$$

For thermoEMF the following relation is true:

$$\alpha = \frac{\int_0^1 \{(\alpha_m/\kappa_m)v(y) + (\alpha_s/\kappa_s)[1 - v(y)]\}dy}{\int_0^1 \{\kappa_m^{-1}v(y) + \kappa_s^{-1}[1 - v(y)]\}dy}. \tag{10}$$

Approximation of the temperature dependences of thermoelectric characteristics of material and metal

To calculate the temperature dependences of contact resistance, we will need the temperature dependences of thermoelectric characteristics of TEM and metal. This approximation can be done in two ways, namely by construction of regression models on the basis of experimental data, or purely by calculation, on the basis of certain model assumptions of the microscopic mechanisms of charge and heat transfer in material. In this paper we use the second way.

We start with the thermoelectric characteristics of TEM. Let at some temperature T_0 we know its thermoelectric parameters, namely the thermoEMF α_{s0}, the electrical conductivity σ_{s0} and the thermal conductivity κ_{s0}. To construct their temperature dependences, using this data we make the following model assumptions:

1) zone spectrum of carriers in TEM is parabolic and isotropic with temperature independent effective mass;
2) quasi-elastic scattering of carriers in relevant temperature region occurs on the deformation potential of acoustic phonons with energy independent cross section and mean free path inversely proportional to temperature;
3) lattice thermal conductivity of semiconductor is determined by phonon-phonon scattering with umklapp and is inversely proportional to temperature.

Provided that these assumptions are valid, the carrier scattering index $r = –0.5$. Taking into account its value, the construction of the necessary temperature dependences on the basis of known general relations [33] is carried out in the following order.

From the relation for the thermoEMF

$$\alpha_{s0} = \frac{k}{e}\left[\frac{2F_1(\eta_0)}{F_0(\eta_0)} - \eta_0\right] \tag{11}$$

we find a reduced chemical potential η_0 of carrier gas at temperature T_0.

Using the condition of carrier concentration constancy, from the equation

$$\frac{T^{1.5}F_{0.5}(\eta)}{T_0^{1.5}F_{0.5}(\eta_0)} = 1 \tag{12}$$

we determine the temperature dependence of reduced chemical potential η of carrier gas on temperature T in given temperature range.

From the relation

$$\alpha_s = \frac{k}{e}\left[\frac{2F_1(\eta)}{F_0(\eta)} - \eta\right] \tag{13}$$

we determine the temperature dependence of the thermoEMF of TEM.

From the relation

$$L_s(\eta) = \left(\frac{k}{e}\right)^2\left[\frac{3F_2(\eta)}{F_0(\eta)} - \frac{4F_1^2(\eta)}{F_0^2(\eta)}\right] \tag{14}$$

we determine the temperature dependence of the Lorentz number of TEM.

The temperature dependence of electrical conductivity of TEM for the above model assumptions is determined as:

$$\sigma_s = \sigma_{s0}\left(\frac{T_0}{T}\right)^{1.5}\frac{F_0(\eta)F_{0.5}(\eta_0)}{F_{0.5}(\eta)F_0(\eta_0)}\,. \tag{15}$$

The temperature dependence of thermal conductivity with regard to everything mentioned above is determined as:

$$\kappa_s = \sigma_s L_s(\eta)T + [\kappa_{s0} - \sigma_{s0}L_s(\eta_0)T_0]\frac{T_0}{T}\,. \tag{16}$$

In formulae (11) – (16), $F_m(\eta)$ denote the Fermi integrals that are determined by the following relation:

$$F_m(\eta) = \int_0^\infty x^m \left[\exp(x-\eta)+1\right]^{-1} dx\,. \tag{17}$$

Relations (11)–(17) completely determine the temperature dependences of the thermoEMF, the electrical conductivity and the thermal conductivity of TEM.

Let us pass to approximation of the temperature dependences of the electrical conductivity, the thermal conductivity and the thermoEMF of metal. We assume that in metal, just as in TEM, scattering of free carriers takes place on the deformation potential of acoustic phonons, and in the real temperature region the mean free path of carriers is inversely proportional to temperature. Then, taking into account strong degeneracy of carriers in metal, the temperature dependence of its electrical conductivity will be determined as [34]:

$$\sigma_m = \sigma_{m0} \cdot (T_0/T), \tag{18}$$

and, therefore, taking into account the Wiedemann-Franz relation, the thermal conductivity of the metal κ_m will be considered to be temperature independent. We will also consider the thermoEMF of the metal α_m to be independent of temperature.

Results of calculation of the temperature dependences of thermoelectric characteristics of the TEM-metal transient contact layer and their discussion

The temperature dependences of the electrical and thermal contact resistances, the thermoEMF and the dimensionless thermoelectric figure of merit of the TEM-metal transient contact layer for bismuth telluride-nickel pair obtained in the framework of the calculation procedure described above, provided that the uneven distribution of the metal atoms in the layer is preserved, are shown in Figs. 1–7.

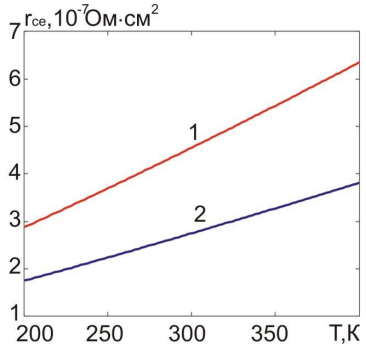

Fig.1. Temperature dependences of electrical contact resistance at transient layer thickness of 20 μm: 1 – A=0; 2 – A=1.

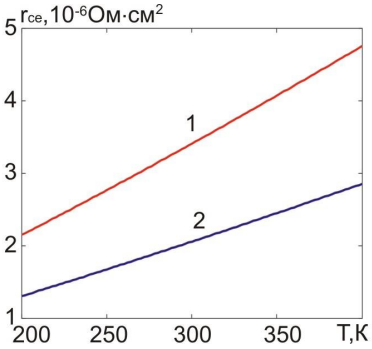

Fig.2. Temperature dependences of electrical contact resistance at transient layer thickness of 150 μm: 1 – A=0; 2 – A=1.

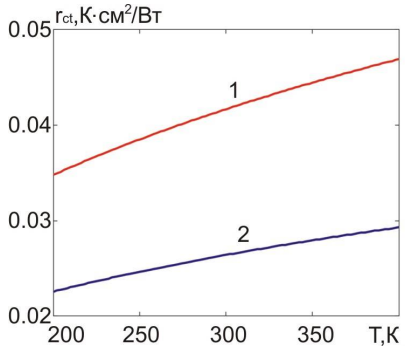

Fig.3. Temperature dependences of thermal contact resistance at transient layer thickness of 20 μm: 1 – A=0; 2 – A=1.

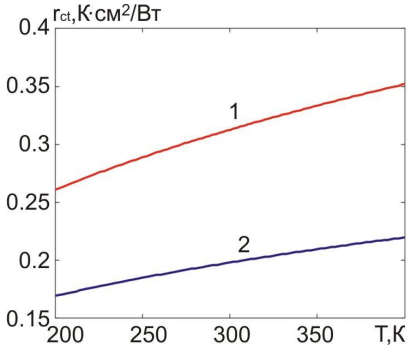

Fig.4. Temperature dependences of thermal contact resistance at transient layer thickness of 150 μm: 1 – A=0; 2 – A=1.

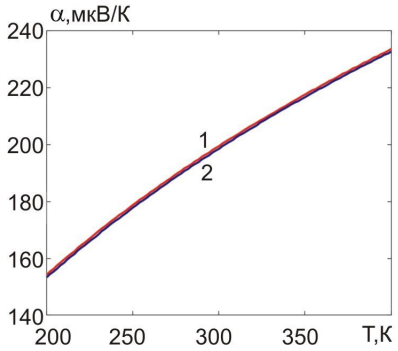

Fig.5. Temperature dependences of transient layer thermoEMF: 1 – A=0; 2 – A=1.

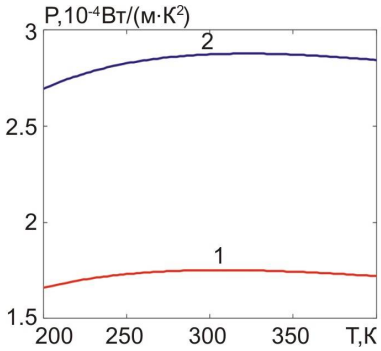

Fig.6. Temperature dependences of transient layer power factor: 1 – A=0; 2 – A=1.

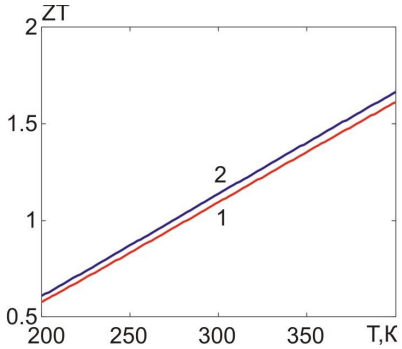

Fig.7. Temperature dependences of transient layer dimensionless thermoelectric figure of merit: 1 – A=0; 2 – A=1.

When plotting, the following material parameters for 300K were taken: σ_m=1.25·10^5 S/cm, σ_s=800 S/cm, κ_m=92 W /(m·K), κ_s=1.4 W /(m·K), α_m= – 23 μV/K, α_s= 200 μV/K, and, besides, A_m=58.5, A_s=801, ρ_m=9100 kg/m^3, ρ_s=7700 kg/m^3. It can be seen from the figures that in the temperature range studied, the electrical and thermal contact resistances, the thermoEMF, and the dimensionless thermoelectric figure of merit of transient layer increase, and the power factor has a maximum in the range of 300–350 K. Such temperature dependences can be explained by an increase in the resistivities of metal and semiconductor, a decrease in their thermal conductivity, and an increase in the thermoEMF of semiconductor with a rise in temperature. With an increase in the thickness of transient layer, the electrical and thermal contact resistances increase in proportion to this thickness. The presence of a maximum in the temperature dependence of power factor is explained by two competing processes: an increase in the thermoEMF and a decrease in TEM electrical conductivity with a rise in temperature. It should be noted that the thermoEMF of transient layer is mainly determined by the semiconductor due to the fact that thermal conductivity of metal is significantly greater than thermal conductivity of semiconductor.

In addition, it can be seen from the figures that with increasing parameter A, that is, the intensity of metal atoms entering transient layer, the thermal and electrical contact resistances, as well as the thermoEMF decrease, and the power factor and the dimensionless thermoelectric figure of merit increase. On the whole, in the studied ranges of temperature, the intensity of metal entering transient layer, and the transient layer thickness, the electrical contact resistance varies from 1.8·10^{-7} to 4.8·10^{-6} Ohm·cm^2, and the thermal contact resistance varies from 0.022 to 0.35 K·cm^2/W, the thermoEMF - from 155 to 235 μV/K, the power factor - from 1.6·10^{-4} до 2.9·10^{-4} W/(m·K^2), the dimensionless thermoelectric figure of merit - from 0.55 to 1.7.

4. Effect of levelling of metal concentration in transient layer on the temperature dependences of its thermoelectric characteristics

The above results were obtained on the assumption that the distribution of the volume fraction of metal in transient layer is subject to relation (4). However, the most intense supply of metal atoms into transient layer occurs directly during contact. Further, especially at low temperatures, this intensity decreases significantly and the uneven distribution of metal in transient layer is levelled. Therefore, it is worthwhile to study the effect of this levelling on the temperature dependences of thermoelectric characteristics of transient layer. After levelling, the average steady volume fraction of metal in transient layer will be determined as follows:

$$v_{ma} = \int_0^1 \frac{(A_m/\gamma_m)\left[1-(1-A)y-Ay^2\right]}{(A_m/\gamma_m)\left[1-(1-A)y-Ay^2\right]+(A_s/\gamma_s)\left[(1-A)y+Ay^2\right]}dy, \qquad (19)$$

So, the steady electrical conductivity of transient layer without regard to percolation theory will be determined as:

$$\sigma_a = \sigma_s + (\sigma_m - \sigma_s)v_{ma}, \tag{20}$$

and its electrical contact resistance as:

$$r_{ce} = h/\sigma_a . \tag{21}$$

The steady thermal conductivity of transient layer will be determined as:

$$\kappa_a = \kappa_s + (\kappa_m - \kappa_s)v_{ma}, \tag{22}$$

and its thermal contact resistance as:

$$r_{ce} = h/\kappa_a . \tag{23}$$

For the thermoEMF of transient layer the following relation is valid:

$$\alpha_l = \frac{(\alpha_m/\kappa_m)v_m + (\alpha_s/\kappa_s)(1-v_m)}{v_m/\kappa_m + (1-v_m)/\kappa_s}. \tag{24}$$

The results of calculations of the temperature dependences of thermoelectric characteristics of transient layer obtained in case of uniform distribution of metal concentration therein are presented in Figs.8–14.

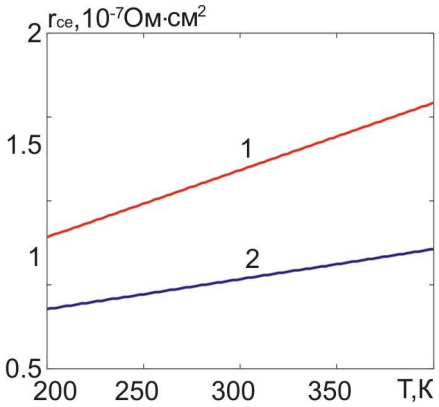

Fig.8. Temperature dependences of electrical contact resistance after levelling of metal concentration at transient layer thickness of 20 μm: 1 – A=0; 2 – A=1.

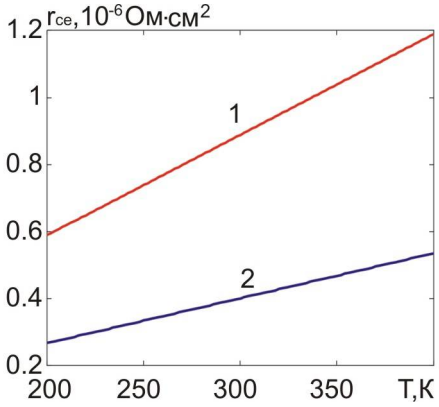

Fig.9. Temperature dependences of electrical contact resistance after levelling of metal concentration at transient layer thickness of 150 μm: 1 – A=0; 2 – A=1.

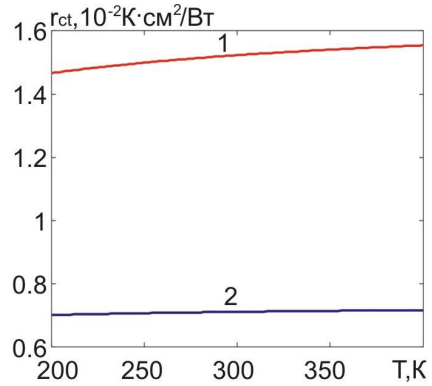

Fig.10. Temperature dependences of thermal contact resistance after levelling of metal concentration at transient layer thickness of 20 μm: 1 – A=0; 2 – A=1.

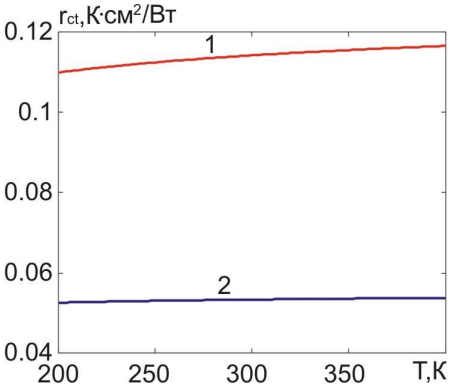

Fig.11. Temperature dependences of thermal contact resistance after levelling of metal concentration at transient layer thickness of 150 μm: 1 – A=0; 2 – A=1.

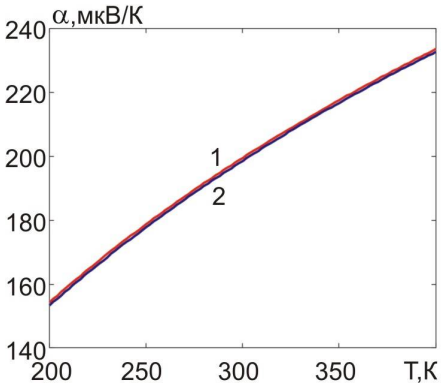

Fig.12. Temperature dependences of transient layer thermoEMF after levelling of metal concentration: 1 – A=0; 2 – A=1.

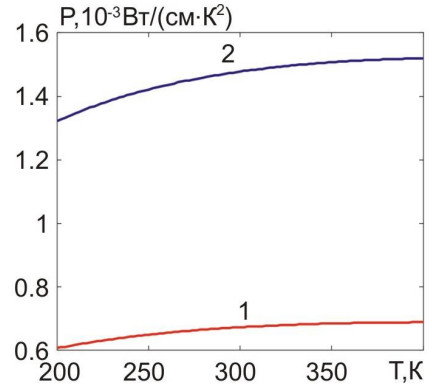

Fig.13. Temperature dependences of transient layer power factor after levelling of metal concentration: 1 – A=0; 2 – A=1.

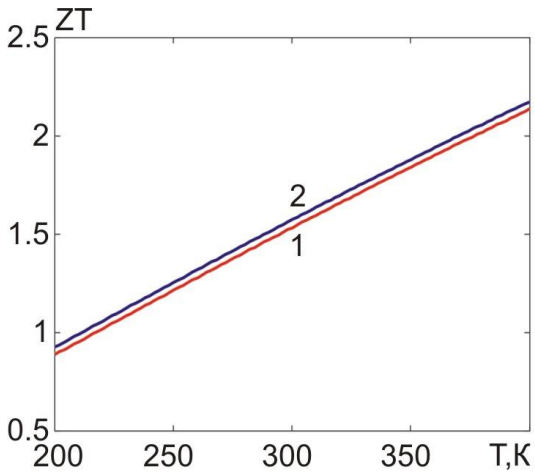

Fig.14. Temperature dependences of transient layer dimensionless thermoelectric figure of merit after levelling of metal concentration: 1 – A=0; 2 – A=1.

It can be seen from the figures that after levelling of metal concentration in the bulk of transient layer, the electrical and thermal contact resistances at all temperatures essentially decrease, the thermoEMF power practically does not change, and the power factor and thermoelectric figure of merit essentially increase. In contrast to the case of an uneven distribution of concentration, after its levelling in the studied temperature range, the power factor does not have a maximum, but is a growing function of temperature.

As regards the effect of parameter A, that is, the intensity of metal entering transient layer, on the thermoelectric properties of transient layer, after the concentration is levelled, the same tendency remains as with its uneven distribution.

In general, in the studied ranges of temperature, the intensity of metal entering transient layer and the thickness of transient layer after levelling metal concentration the electrical contact resistance varies from $8\cdot10^{-8}$ to $1.2\cdot10^{-6}$ Ohm·cm^2, the thermal contact resistance – from $7\cdot10^{-3}$ to 0.12 K·cm^2/W, the thermoEMF – from 155 to 235 V/K, the power factor – from $6\cdot10^{-4}$ to 1.5 $5\cdot10^{-3}$ W/(m·K^2), the dimensionless thermoelectric figure of merit – from 0.8 to 2.2. Thus, after the concentration is levelled, the electrical contact resistance drops by a factor of 2.25 – 4, the thermal contact resistance drops by a factor of 3, the thermoEMF is practically unvaried, the power factor grows by a factor of 3.75 – 5.3, the thermoelectric figure of merit increases 1.5 times.

Note that when designing thermoelectric energy converters, such parameters of transient contact layers as power factor and thermoelectric figure of merit do not have self-importance, but they may be of some interest for the integral evaluation of the contact structures.

It is clear that the results obtained can be considered valid only when nickel does not form bismuth telluride intermetallic compounds. But according to the data of [23], this is basically true.

Effect of contact resistance on the efficiency of thermoelectric generator module

The above temperature dependences of the electrical and thermal contact resistances were used to calculate the efficiency of thermoelectric generator modules with the height of thermoelectric legs 3 and 1.5 mm, respectively. The calculations were performed by methods of object-oriented simulation in Comsol Multiphysics software environment.

For this purpose a physical model of thermoelectric generator module was considered which is shown in Fig.15.

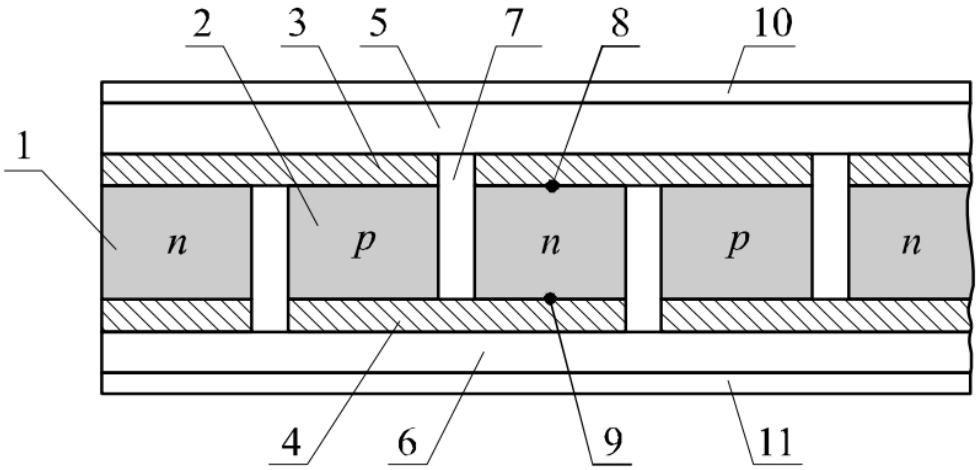

Fig. 15. Physical model of thermoelectric generator module. 1 – n-type leg; 2 – p-type leg; 3, 4 – electrical interconnects; 5, 6 – ceramic plates; 7 – gas; 8, 9 – electrical contacts between legs and interconnect plates; 10 – thermal contact between ceramic plate and hot thermostat; 11 – thermal contact between ceramic plate and cold thermostat.

The distribution of temperature and electrical potential in the module was found from the system of differential equations with respect to temperature T and electrochemical potential U. These equations were obtained on the basis of the law of energy conservation which is given by the following two equations:

$$\nabla \vec{w} = 0\,, \tag{25}$$

$$\vec{w} = \vec{q} + U\vec{j}\,. \tag{26}$$

In formulae (25) and (26), $\vec{j}$ – electric current density, $\vec{q}$ – heat flux density:

$$\vec{q} = -\kappa \nabla T + \Pi \vec{j}\,, \tag{27}$$

where Π is the Peltier coefficient, κ is thermal conductivity.

$$\Pi = \alpha T, \tag{28}$$

where α is the Seebeck coefficient, T is temperature.

The electric current density is found from the equation

$$\vec{j} = -\sigma \nabla U - \sigma \alpha \nabla T\,, \tag{29}$$

where σ is the electrical conductivity.

Substituting (26), (27) into (25), we obtain

$$-\nabla\left(\kappa \nabla T\right) + \left(\nabla \Pi + \nabla U\right)\vec{j} = 0\,. \tag{30}$$

From expression (30), using (28) and (29), we obtain the following equation to find the distributions of temperature and potential:

$$-\nabla\left[\left(\sigma\alpha^2T+\kappa\right)\nabla T\right]-\nabla\left(\sigma\alpha T\nabla U\right)-\sigma\left[\left(\nabla U\right)^2+\alpha\nabla T\nabla U\right]=0. \quad (31)$$

To obtain the second equation, we will use the law of conservation of electrical charge:

$$\nabla\vec{j}=0. \quad (32)$$

Substituting (29) into (32), we obtain the following equation:

$$\nabla\left(\sigma\alpha\nabla T\right)+\nabla\left(\sigma\nabla U\right)=0. \quad (33)$$

System (31), (33) is a system of differential equations with variable second-order partial differential coefficients, which describes the distribution of temperature and potential in an inhomogeneous thermoelectric medium. A feature of the system of equations (31), (33) is that the parameters α, σ, κ depend on the spatial coordinates x, y, z both directly and implicitly through the temperature T (x, y, z). This leads to the fact that it becomes inevitable to use numerous computer methods to solve equations of this kind.

In a computer model, the thermoelectric field is described by a two-element column matrix in the functional space of twice differentiable functions, namely, the coordinate dependences of temperature and potential:

$$M=\begin{pmatrix}T(x,y,z)\\U(x,y,z)\end{pmatrix}. \quad (34)$$

Matrix M satisfies one matrix differential equation

$$\nabla\left(c\nabla M\right)=f, \quad (35)$$

whose components are equations (31) and (33) if the matrix nonlinear coefficients of equation (35) have the form

$$c=\begin{pmatrix}\sigma\alpha^2T+\kappa & \sigma\alpha T\\ \alpha\sigma & \sigma\end{pmatrix}, f=\begin{pmatrix}\sigma\left[\left(\nabla U\right)^2+\nabla T\nabla U\right]\\ 0\end{pmatrix}. \quad (36)$$

A system of equations of the form (35) with allowance for (36) is solved for each of the layers that make up the thermoelectric module. For this, we additionally introduce the boundary conditions for the continuity of temperature, electric potential, heat flux, and electric current density at the boundaries of the layers. In addition, for reasons of optimality of the conditions under which the thermoelement operates, and which are determined from the requirement to achieve the maximum value of the efficiency, the potentials on the switching electrodes and the temperatures of the "hot" and "cold" thermostats are set. Therefore, the potentials on the switching electrodes of one of the legs are 0 and 0.0573 V, on the second - 0.0573 and 0.1146 V, and the temperatures of the "cold" and "hot" thermostats are 273 and 573 K, respectively.

The impact of the electrical and thermal contact resistances is taken into account in the physical model in the framework of two approaches. The first is that the contact layer is not explicitly introduced into the physical model, but its electrical conductivity and thermal conductivity are considered to be known from experiment or, in this case, temperature functions preliminarily calculated by calculation. Then, the proportionality of the electrical and thermal contact resistances to the layer thickness is taken into account. The second approach is that a contact layer with temperature-dependent thermal conductivity and electrical conductivity, taking into account its thickness, is explicitly introduced into the physical model. The thermoEMF of the contact layer at this stage of research is not taken into account.

Such mathematical description allows solving the above described system of equations for temperature and potential in Comsol Multiphysics simulation environment. The results of solving Eq.(11)

are three-dimensional temperature and electrical fields in given geometry of thermoelectric module. Their examples for one thermoelement which is part of the module with the height of leg 3 mm are shown in Figs. 16, 17. Knowing these fields, it is easy to calculate the basic energy characteristics of the module.

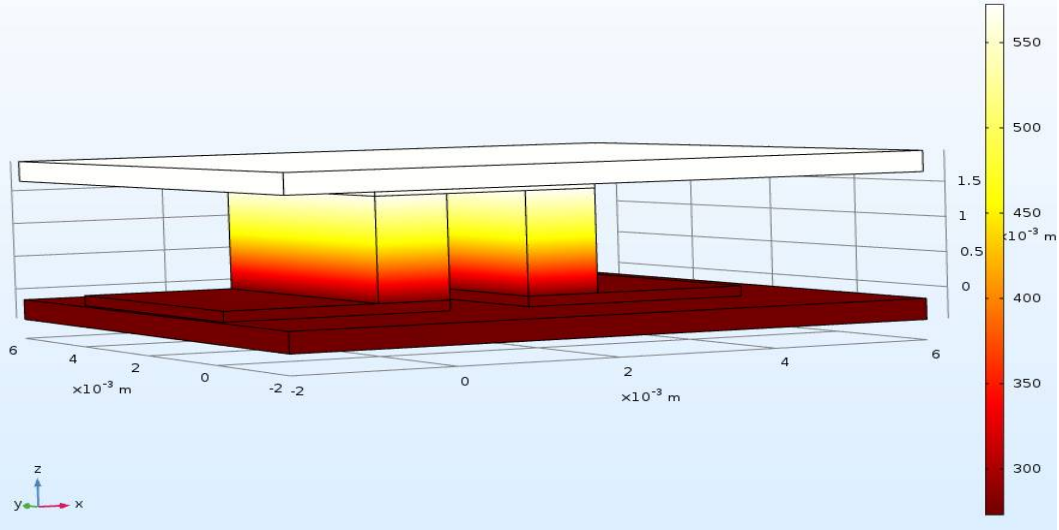

Fig.16. Temperature field in thermoelement

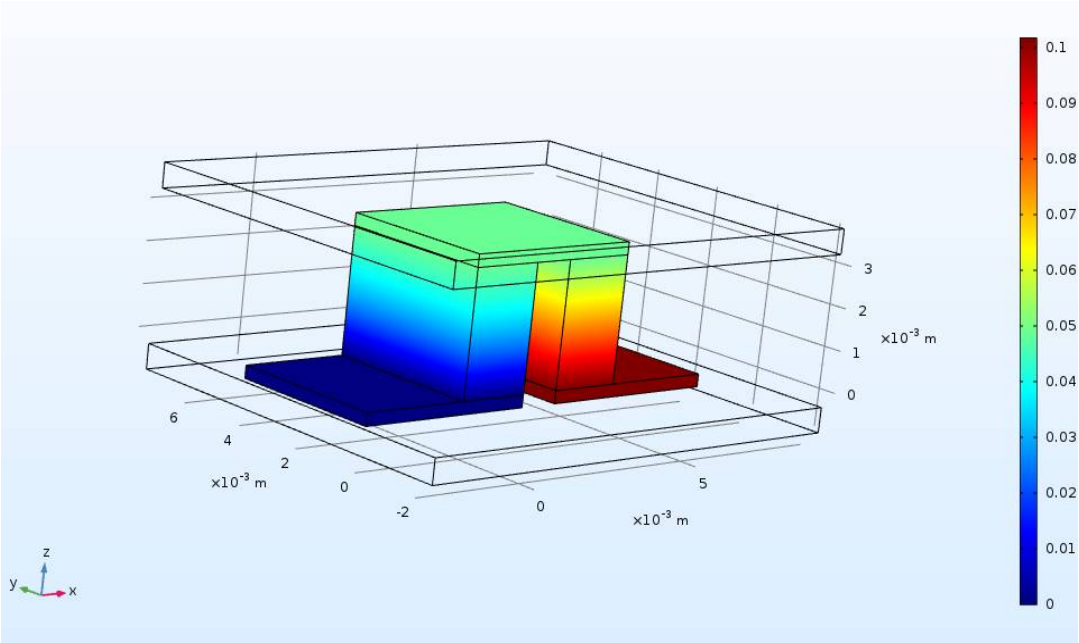

Fig.17.Electrical potential distribution in thermoelement

The results of these calculations are presented in Figs.18 – 21.

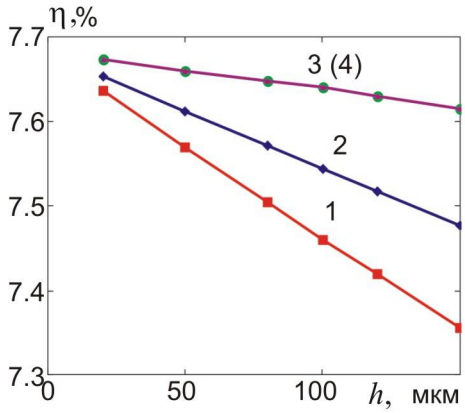

Fig.18.Dependence of generator module efficiency with the height of leg 3 mm on transient layer thickness for the case when contact resistance is considered to be a lumped parameter:1 – A=0, the distribution of metal atoms in transient layer is uneven; 2 – A=1, the distribution of metal atoms in transient layer is uneven; 3 – A=0, the distribution of metal atoms in transient layer is uniform;4 – A=1, the distribution of metal atoms in transient layer is uniform.

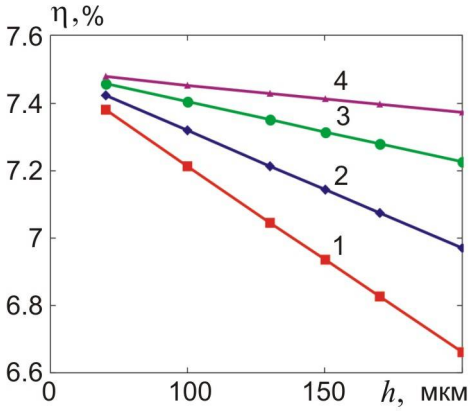

Fig.19.Dependence of generator module efficiency with the height of leg 1.5 mm on transient layer thickness for the case when contact resistance is considered to be a lumped parameter:1 – A=0, the distribution of metal atoms in transient layer is uneven; 2 – A=1, the distribution of metal atoms in transient layer is uneven; 3 – A=0, the distribution of metal atoms in transient layer is uniform;4 – A=1, the distribution of metal atoms in transient layer is uniform.

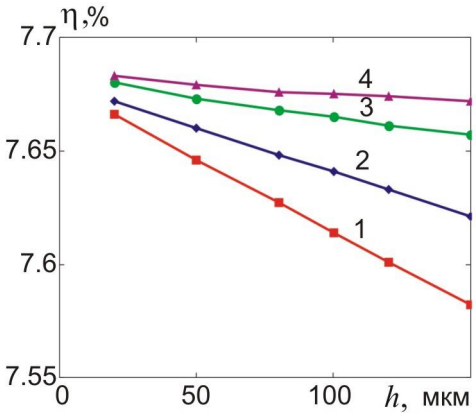

Fig.20.Dependence of generator module efficiency with the height of leg 3 mm on transient layer thickness for the case when transient layer is explicitly introduced into model:1 – A=0, the distribution of metal atoms in transient layer is uneven; 2 – A=1, the distribution of metal atoms in transient layer is uneven; 3 – A=0, the distribution of metal atoms in transient layer is uniform;4 – A=1, the distribution of metal atoms in transient layer is uniform.

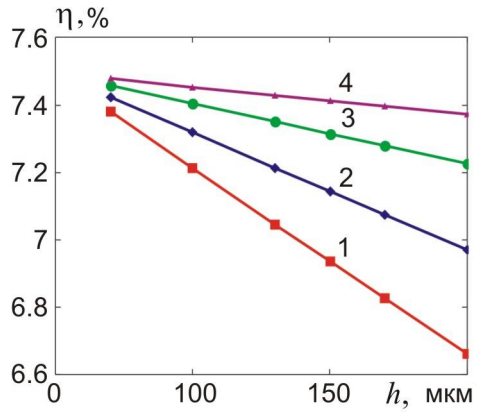

Fig.21.Dependence of generator module efficiency with the height of leg 1.5 mm on transient layer thickness for the case when transient layer is explicitly introduced into model:1 – A=0, the distribution of metal atoms in transient layer is uneven; 2 – A=1, the distribution of metal atoms in transient layer is uneven; 3 – A=0, the distribution of metal atoms in transient layer is uniform;4 – A=1, the distribution of metal atoms in transient layer is even.

Note that in this case, the thermoEMF of transient layer was considered to be zero.

It can be seen from the figures that the efficiency of the thermoelement in the mode of electric energy generation is maximum when the distribution of metal atoms in transient layer is uniform. In addition, other things being equal, it is the greater, the greater the intensity of the source from which the metal enters transient layer. In the case of uneven distribution of metal atoms in transient layer, the efficiency decreases with increasing transient layer thickness the more, the smaller the height of the thermoelectric leg. In general, in the considered range of thermoelectric leg heights and layer thicknesses, the efficiency changes from 6.4 to 7.7% when the contact layer is explicitly introduced into the model, and from 6.6 to 7.7% when the contact resistance is considered to be a lumped parameter. In the case when transient layer is introduced into model, the efficiency after levelling the distribution of metal atoms in transient layer depends only slightly on the intensity of the source from which a steady-state diffusion of metal to TEM occurs.

Conclusions

1. Without taking into account the formation of clusters in transient layer, the temperature dependences of the electrical and thermal contact resistances, the thermoEMF, the power factor and the thermoelectric figure of merit of bismuth telluride-nickel transient contact layers were calculated on the assumption that carrier scattering in semiconductor and metal occurs on the deformation potential of acoustic phonons, the thermal conductivity of metal is determined by electron gas, and the lattice thermal conductivity of semiconductor – by phonon-phonon scattering with umklapp. In this case it was believed that nickel does not form new phases with bismuth telluride.
2. It is shown that both with uneven and uniform distribution of metal atoms in transient layer, the electrical and thermal contact resistances, the thermoEMF and the dimensionless thermoelectric figure of merit of transient layer are growing functions of temperature and the intensity of metal atoms entering transient layer during contact creation.
3. Power factor in the temperature range under study is a growing function of the intensity of metal atoms entering transient layer, and at the same time has a maximum on the temperature dependence in case of uneven distribution of metal atoms in transient layer. However, it becomes a monotonically growing function of temperature in case of levelling the concentration of metal atoms in transient layer.
4. In the case of uneven distribution of metal atoms in the temperature range of 200 – 400 K, the intensity

of metal atoms entering transient layer, which corresponds to a change in parameter *A* from 0 to 1 and the thickness range of transient layer from 20 to 150 μm, the electrical contact resistance changes from $1.8 \cdot 10^{-7}$ to $4.8 \cdot 10^{-6}$ Ohm·cm^2, the thermal contact resistance – from 0.022 to 0.35 K·cm^2/W, the thermoEMF – from 155 to 235 μV/K, the power factor – from $1.6 \cdot 10^{-4}$ to $2.9 \cdot 10^{-4}$ W/(m·K^2), the dimensionless thermoelectric figure of merit – from 0.55 to 1.7.

5. In the case of levelling the distribution of metal atoms in transient layer, the electrical contact resistance decreases by a factor of 2.25 – 4, the thermal contact resistance decreases by a factor of 3, the thermoEMF is practically unvaried, the power factor increases by a factor of 3.75 – 5.3, the thermoelectric figure of merit grows by a factor of 1.5 as compared to the case of uneven distribution.
6. Studies of the effect of transient contact layer without clusters on the efficiency of thermoelement in generation mode have shown that, all other things being equal, if the influence of the thermoEMF of transient layer is ignored, in the considered range of thermoelectric leg heights and layer thicknesses in the case when a contact layer is explicitly introduced into the model, the efficiency varies from 6.4 to 7.7%. However, if contact resistance is considered to be a lumped parameter, the efficiency changes from 6.6 to 7.7%. In the case when transient layer is introduced into the model, the efficiency after levelling the distribution of metal atoms in transient layer depends only slightly on the intensity of the source from which steady diffusion of metal into TEM occurs, whereas in the case when contact resistance is considered to be a lumped parameter, this dependence is much stronger.

References

1. Aswal D.K., Basu R., Singh A. (2016). Key issues in development of thermoelectric power generators: high figure-of-merit materials and their highly conducting interfaces with metallic interconnects. *Energy Convers. Manag.,* 114, 50-67. http://refhub.elsevier.com/S2468-6069(18)30133-3/sref1
2. Anatychuk L.I., Kuz R.V. (2012). The energy and economic parameters of *Bi-Te* based thermoelectric generator modules for waster heat recovery. *J.Thermoelectricity*, 4, 75-82.
3. Drabkin I.A., Osvensky V.B., Sorokin A.I., Panchenko V.P., Narozhnaya O.E. (2017). Contact resistance in composite thermoelectric legs. *Semiconductors,* 51(8), 1038-1040.
4. Anatychuk L.I. (2003). *Termoelektrichestvo. Tom 2. Termoelektricheskiie preobrazovateli energii [Thermoelectricity. Vol.2. Thermoelectric power converters]*. Kyiv, Chernivtsi: Institute of Thermoelectricity [in Russian].
5. Semenyuk V. (2001). Thermoelectric micro modules for spot cooling of high density heat sources. *Proc. of 20th International Conference on Thermoelectrics*, 391-396.
6. Semenyuk V.A. (2006). Thermoelectric cooling of electro-optic components. *Thermoelectrics Handbook: Macro to Nano, 58-1 – 58-20. D.M. Rowe (Ed.).* CRC Taylor&Francis.
7. Fleurial J.-P., Snyder G.J., Patel J., et al. (2001). Solid-state power generation and cooling microdevices for distributed system architectures. *Proc of 20th International Conference on Thermoelectrics*, 24-29.
8. Bottner Harald, Nurnus Joachim, Schubert Axel (2006). Miniaturized thermoelectric converters. *Thermoelectrics Handbook, Macro to Nano. D.M. Rowe (Ed.).* CRC Taylor&Francis, 46-1 – 46-18.
9. Crane N. B., Misra P., Murray Jr. J.L., Nolas G.S. (2009). Self-assembly for integration of microscale thermoelectric coolers. *Journal of Electronic Materials*, 38 (7), 1252-1256.
10. I-Yu Huang, Jr-Ching Linb, Kun-Dian She (2008). Development of low-cost micro-thermoelectric coolers utilizing MEMS technology. *Sensors and Actuators*, A 148, 176–185.

11. Navone C., Soulier M., Plissonnier M., Seiler A.L. (2010). Development of $(Bi,Sb)_2(Te,Se)_3$-based thermoelectric modules by a screen-printing process. *Journal of Electronic Materials*, 39 (9), 1755-1759.
12. Goncalves L.M., Couto C., Alpuim P., Correia J.H. (2008). Thermoelectric micro converters for cooling and energy-scavenging systems. *J. Micromech. Microeng.*, 18, 064008, 1-5.
13. Misra P., Nagaraju J. (2004). Test facility for simultaneous measurement of electrical and thermal contact resistance. *Rev. Sci. Instr*., 75, 2625-2630 (doi 10.1063/1.1775316).
14. Maheshappa H.D., Nagaraju J., KrishnaMurthu N.V. (1998). A facility for electrical contact resistance measurement. *Rev. Sci. Instr*., 69, 534-1539 (doi 10.1063/1.1148810).
15. Deepak, Krishna H. (2007). Measurement of small specific contact resistance of metals with resistive semiconductors. *J. El. Mat*., 36, 598-605 (doi 10.1007/s11664-007-0091-y).
16. Gupta R.P., McCarty R., Sharp J. (2014). Practical contact resistance measurement method for bulk Bi_2Te_3 based thermoelectric devices. *J. El. Mat*., 43 (6), 1608-1612.
17. Kim Y., Yoon G., Park S.H. (2016). Direct contact resistance evaluation of thermoelectric legs. *Experimental Mechanics*, 56 (5), 861-869. https://doi.org/10.1007/s11340-016-0131-8-
18. Alieva T.D., Barkhalov B.Sh., Abdinov D.Sh. (1995). Struktura i elektricheskiie svoistva granits razdela kristallov $Bi_{0.5}Sb_{1.5}Te_3$ i $Bi_2Te_{2.7}Se_3$ s nekotorymi splavami [Structure and electrical properties of interfaces between $Bi_{0.5}Sb_{1.5}Te_3$ and $Bi_2Te_{2.7}Se_3$ crystals with certain alloys]. *Neorganicheskiie Materialy – Inorganic Materials*, 31 (2), 194-198.
19. Dzhamalov N.A., Barkhalov B.Sh., Salaiev E.Yu., Gasanov N.A., Abdinov D.Sh.(1983). *Neorganicheskiie Materialy – Inorganic Materials*, 19(4), 593-595.
20. Alieva T.D., Akhundova N.M., Dzhamalov N.A., et al. (1985). *Reports of the Academy of Sciences of Azerbaijan SSR,* 41(12), 18-20.
21. Kuznetsov G.D., Polystanskiy Y.G., Evseev V.A. (1995). The metallization of the thermoelement branches by ionic sputtering of the nickel and cobalt. *Proc of the XIV International Conference on Thermoelectrics (St.Petersburg, June 27-30, 1995)* (p.166-167).
22. Astakhov M.V., Bublik V.T., Karataiev V.V., et al. (2004). Vliianiie protsessa nikelirovaniia na strukturu i adhesionnyie svoistva poverkhnostnykh sloiov termoelektricheskogo materiala na osnove khalkogenidov Bi i Sb. [The influence of nickel plating process on the structure and adhesion properties of surface layers of thermoelectric material based on Bu and Sb charlcogenides]. In: *"Thermoelectrics and their Application" (Saint-Petersburg, 2004)* (p.243-248).
23. Bublik V.T., Voronin A.I., Ponomarev V.F., Tabachkova N.Yu. (2012). Izmeneniie struktury prikontaknoi oblasti termoelektricheskikh materialov na osnove telluride vismuta pri povyshennykh temperaturakh [Change in the structure of near-contact area of thermoelectric materials based on bismuth telluride at elevated temperatures]. *Izvestiia vysshykh uchebnykh zavedenii.* Materaily Elektronnoi Tekhniki - *News of Higher Educational Institutions.* Materials of Electronic Technique, 2, 17-20 [in Russian].
24. Belonogov E.A., Dybov V.A., Kostiuchenko A.V., et al. Kondensirovannyie sredy i mezhfaznyie granitsy [Condensed media and interphase boundaries], Vol.19, №4, p.479-488.
25. Gupta Rahul P., Xiong K., White J.B., Cho Kyeongjae, Alshareef H.N., Gnade B.E. (2010). Low resistance ohmic contacts to Bi2Te3 using Ni and Co metallization. *Journal of the Electrochemical Society,* 157 (6), H666-H670, 2010. DOI: 10.1149/1.3385154
26. Ngan Hoang Pham, Nader Farahi, Hasbuna Kamila, Aryan Sankhla, Sahar Ayachi, Eckhard Müller, Johannes de Boor (2019). Ni and Ag electrodes for magnesium silicide based thermoelectric generators. *Materials Today Energy*, 11 97e105. https://doi.org/10.1016/j.mtener.2018.10.016.

27. Nikirsa D.D. (1987). Fizicheskiie osobennosti mikrominiaturizatsii polyprovodnikovykh okhlazhdaiushchikh termoelementov [Physical features of microminiaturization of semiconductor cooling thermoelements]. Candidate's thesis (Tech.sciences). Chernivtsi [in Russian].
28. Bartkowiak M., Mahan G.D. (2001). Heat and electricity transport through interfaces, in: *Recent Trends in Thermoelectric Materials, vol. II, Semiconductors and Semimetals*, vol. 70. New York: Academic Press.
29. Sze S.M. (1985). *Semiconductor Devices - Physics and Technology*, John Wiley & Sons.
30. Goldberg Yu.A. (1994). Ohmic contact metal-semiconductor AIIIBV: creation methods and properties. *Semiconductors*, 28(10), 1681-1698.
31. Da Silva L.W., Kaviany M. (2004). Microthermoelectric cooler: interfacial effects on thermal and electrical transport. *International Journal of Heat and Mass Transfer*, 47(10-11), 2417–2435.
32. Anatychuk L.I., Dugaev V.K., Litvinov V.I., Volkov V.L. (1994). Contact resistance between metal and thermoelectric material. *J. Thermoelectricity*, 1, 70-77.
33. Goltsman B.M., Kudinov I.A., Smirnov I.A. (1972). *Poluprovodnikovyie termoelektricheskiie materaily na osnove Bi_2Te_3 [Semiconductor thermoelectric materials based on Bi_2Te_3]*. Moscow: Nauka [in Russian].
34. Lifshits E.M., Pitaevskii L.P. (1979). *Fizicheskaia kinetika [Physical kinetics]*. Moscow: Nauka [in Russian].

Submitted 17.04.2019

Горський П.В. *док. фіз.-мат. наук*[1,2]
Мицканюк Н.В.[1,2]

[1]Інститут термоелектрики НАН і МОН України,
вул. Науки, 1, Чернівці, 58029, Україна;
e-mail: anatych@gmail.com;
[2]Чернівецький національний університет
ім. Юрія Федьковича, вул. Коцюбинського 2,
Чернівці, 58000, Україна

ПРО ТЕМПЕРАТУРНІ ЗАЛЕЖНОСТІ ТЕРМОЕЛЕКТРИЧНИХ ХАРАКТЕРИСТИК ПЕРЕХІДНОГО ШАРУ ТЕРМОЕЛЕКТРИЧНИЙ МАТЕРІАЛ-МЕТАЛ БЕЗ УРАХУВАННЯ ЯВИЩА ПЕРКОЛЯЦІЇ

Розрахунковим шляхом отримано основні співвідношення, які визначають температурні залежності термоелектричних характеристик перехідних контактних шарів термоелектричний матеріал-метал без урахування теорії протікання. Конкретні кількісні результати та графіки температурних залежностей електричного та теплового контактних опорів, термоЕРС, фактору потужності та безрозмірної термоелектричної ефективності наведено для контактної пари телурид вісмуту – нікель. Встановлено, що разі нерівномірного розподілу атомів металу в інтервалі температур 200 – 400 К, інтенсивності надходження атомів металу у перехідний шар, яка відповідає зміні розподілу атомів металу за товщиною перехідного шару від лінійного до квадратичного та інтервалі товщин перехідного шару від 20 до 150 мкм електричний контактний опір змінюється від $1.8\cdot10^{-7}$ до $4.8\cdot10^{-6}$ Ом·см^2, тепловий контактний опір – від 0.022 до 0.35 К·см^2/Вт, термоЕРС – від 155 до 235 мкВ/К, фактор потужності – від $1.6\cdot10^{-4}$ до $2.9\cdot10^{-4}$ Вт/(м·К^2), безрозмірна термоелектрична ефективність – від 0.55 до 1.7. Бібл. 34, рис. 21.

Ключові слова: контакт термоелектричний матеріал – метал, приконтактний перехідний шар, електричний контактний опір, тепловий контактний опір, термоЕРС, фактор потужності, безрозмірна термоелектрична ефективність, температурні залежності.

Горский П.В., *док. физ-мат. наук*[1,2]
Мыцканюк Н.В.[1,2]

[1]Институт термоэлектричества НАН и МОН Украины, ул. Науки, 1,
Черновцы, 58029, Украина, *e–mail: anatych@gmail.com;*
[2]Черновицкий национальный университет
им. Юрия Федьковича, ул. Коцюбинского, 2,
Черновцы, 58012, Украина

О ТЕМПЕРАТУРНЫХ ЗАВИСИМОСТЯХ ТЕРМОЭЛЕКТРИЧЕСКИХ ХАРАКТЕРИСТИК ПЕРЕХОДНОГО СЛОЯ ТЕРМОЭЛЕКТРИЧЕСКИЙ МАТЕРИАЛ-МЕТАЛЛ БЕЗ УЧЕТА ЯВЛЕНИЯ ПЕРКОЛЯЦИИ

Расчетным путем получены основные соотношения, определяющие температурные зависимости термоэлектрических характеристик переходных контактных слоев термоэлектрический материал-металл без учета теории протекания. Конкретные количественные результаты и графики температурных зависимостей электрического и теплового контактных сопротивлений, термоЭДС, фактора мощности и безразмерной термоэлектрической эффективности приведены для контактной пары телурид висмута - никель. Установлено, что в случае неравномерного распределения атомов металла в интервале температур 200 - 400 К, интенсивности поступления атомов металла в переходной слой, которая отвечает изменению распределения атомов металла по толщине переходного слоя от линейного к квадратичному в интервале толщин переходного слоя от 20 до 150 мкм электрическое контактное сопротивление изменяется от 1.8· 10^{-7} до 4.8 10^{-6} Ом·см^2, тепловое контактное сопротивление - от 0.022 до 0.35 К·см^2/Вт, термоЭДС - от 155 до 235 мкВ/К, фактор мощности - от 1.6 10^{-4} до 2.9 10^{-4} Вт/(м·К^2), безразмерная термоэлектрическая эффективность - от 0.55 до 1.7. Библ. 34, рис. 20.

Ключевые слова: контакт термоэлектрический материал - металл, приконтактный переходный слой, электрическое контактное сопротивление, тепловое контактное сопротивление, термоЭДС, фактор мощности, безразмерная термоэлектрическая эффективность, температурные зависимости.

References

1. Aswal D.K., Basu R., Singh A. (2016). Key issues in development of thermoelectric power generators: high figure-of-merit materials and their highly conducting interfaces with metallic interconnects. *Energy Convers. Manag.,* 114, 50-67. http://refhub.elsevier.com/S2468-6069(18)30133-3/sref1
2. Anatychuk L.I., Kuz R.V. (2012). The energy and economic parameters of *Bi-Te* based thermoelectric generator modules for waster heat recovery. *J.Thermoelectricity*, 4, 75-82.
3. Drabkin I.A., Osvensky V.B., Sorokin A.I., Panchenko V.P., Narozhnaya O.E. (2017). Contact resistance in composite thermoelectric legs. *Semiconductors,* 51(8), 1038-1040.

4. Anatychuk L.I. (2003). *Termoelektrichestvo. Tom 2. Termoelektricheskiie preobrazovateli energii [Thermoelectricity. Vol.2. Thermoelectric power converters]*. Kyiv, Chernivtsi: Institute of Thermoelectricity [in Russian].
5. Semenyuk V. (2001). Thermoelectric micro modules for spot cooling of high density heat sources. *Proc. of 20th International Conference on Thermoelectrics*, 391-396.
6. Semenyuk V.A. (2006). Thermoelectric cooling of electro-optic components. *Thermoelectrics Handbook: Macro to Nano, 58-1 – 58-20. D.M. Rowe (Ed.).* CRC Taylor&Francis.
7. Fleurial J.-P., Snyder G.J., Patel J., et al. (2001). Solid-state power generation and cooling microdevices for distributed system architectures. *Proc of 20th International Conference on Thermoelectrics*, 24-29.
8. Bottner Harald, Nurnus Joachim, Schubert Axel (2006). Miniaturized thermoelectric converters. *Thermoelectrics Handbook, Macro to Nano. D.M. Rowe (Ed.).* CRC Taylor&Francis, 46-1 – 46-18.
9. Crane N. B., Misra P., Murray Jr. J.L., Nolas G.S. (2009). Self-assembly for integration of microscale thermoelectric coolers. *Journal of Electronic Materials*, 38 (7), 1252-1256.
10. I-Yu Huang, Jr-Ching Linb, Kun-Dian She (2008). Development of low-cost micro-thermoelectric coolers utilizing MEMS technology. *Sensors and Actuators*, A 148, 176–185.
11. Navone C., Soulier M., Plissonnier M., Seiler A.L. (2010). Development of $(Bi,Sb)_2(Te,Se)_3$-based thermoelectric modules by a screen-printing process. *Journal of Electronic Materials*, 39 (9), 1755-1759.
12. Goncalves L.M., Couto C., Alpuim P., Correia J.H. (2008). Thermoelectric micro converters for cooling and energy-scavenging systems. *J. Micromech. Microeng.*, 18, 064008, 1-5.
13. Misra P., Nagaraju J. (2004). Test facility for simultaneous measurement of electrical and thermal contact resistance. *Rev. Sci. Instr*., 75, 2625-2630 (doi 10.1063/1.1775316).
14. Maheshappa H.D., Nagaraju J., KrishnaMurthu N.V. (1998). A facility for electrical contact resistance measurement. *Rev. Sci. Instr*., 69, 534-1539 (doi 10.1063/1.1148810).
15. Deepak, Krishna H. (2007). Measurement of small specific contact resistance of metals with resistive semiconductors. *J. El. Mat*., 36, 598-605 (doi 10.1007/s11664-007-0091-y).
16. Gupta R.P., McCarty R., Sharp J. (2014). Practical contact resistance measurement method for bulk Bi_2Te_3 based thermoelectric devices. *J. El. Mat*., 43 (6), 1608-1612.
17. Kim Y., Yoon G., Park S.H. (2016). Direct contact resistance evaluation of thermoelectric legs. *Experimental Mechanics*, 56 (5), 861-869. https://doi.org/10.1007/s11340-016-0131-8-
18. Alieva T.D., Barkhalov B.Sh., Abdinov D.Sh. (1995). Struktura i elektricheskiie svoistva granits razdela kristallov $Bi_{0.5}Sb_{1.5}Te_3$ i $Bi_2Te_{2.7}Se_3$ s nekotorymi splavami [Structure and electrical properties of interfaces between $Bi_{0.5}Sb_{1.5}Te_3$ and $Bi_2Te_{2.7}Se_3$ crystals with certain alloys]. *Neorganicheskiie Materialy – Inorganic Materials*, 31 (2), 194-198.
19. Dzhamalov N.A., Barkhalov B.Sh., Salaiev E.Yu., Gasanov N.A., Abdinov D.Sh.(1983). *Neorganicheskiie Materialy – Inorganic Materials*, 19(4), 593-595.
20. Alieva T.D., Akhundova N.M., Dzhamalov N.A., et al. (1985). *Reports of the Academy of Sciences of Azerbaijan SSR,* 41(12), 18-20.
21. Kuznetsov G.D., Polystanskiy Y.G., Evseev V.A. (1995). The metallization of the thermoelement branches by ionic sputtering of the nickel and cobalt. *Proc of the XIV International Conference on Thermoelectrics (St.Petersburg, June 27-30, 1995)* (p.166-167).
22. Astakhov M.V., Bublik V.T., Karataiev V.V., et al. (2004). Vliianiie protsessa nikelirovaniia na strukturu i adhesionnyie svoistva poverkhnostnykh sloiov termoelektricheskogo materiala na osnove khalkogenidov Bi i Sb. [The influence of nickel plating process on the structure and adhesion properties

of surface layers of thermoelectric material based on Bu and Sb charlcogenides]. In: *"Thermoelectrics and their Application" (Saint-Petersburg, 2004)* (p.243-248).

23. Bublik V.T., Voronin A.I., Ponomarev V.F., Tabachkova N.Yu. (2012). Izmeneniie struktury prikontaknoi oblasti termoelektricheskikh materialov na osnove telluride vismuta pri povyshennykh temperaturakh [Change in the structure of near-contact area of thermoelectric materials based on bismuth telluride at elevated temperatures]. *Izvestiia vysshykh uchebnykh zavedenii.* Materaily Elektronnoi Tekhniki - *News of Higher Educational Institutions.* Materials of Electronic Technique, 2, 17-20 [in Russian].
24. Belonogov E.A., Dybov V.A., Kostiuchenko A.V., et al. Kondensirovannyie sredy i mezhfaznyie granitsy [Condensed media and interphase boundaries], Vol.19, №4, p.479-488.
25. Gupta Rahul P., Xiong K., White J.B., Cho Kyeongjae, Alshareef H.N., Gnade B.E. (2010). Low resistance ohmic contacts to Bi2Te3 using Ni and Co metallization. *Journal of the Electrochemical Society,* 157 (6), H666-H670, 2010. DOI: 10.1149/1.3385154
26. Ngan Hoang Pham, Nader Farahi, Hasbuna Kamila, Aryan Sankhla, Sahar Ayachi, Eckhard Müller, Johannes de Boor (2019). Ni and Ag electrodes for magnesium silicide based thermoelectric generators. *Materials Today Energy*, 11 97e105. https://doi.org/10.1016/j.mtener.2018.10.016.
27. Nikirsa D.D. (1987). Fizicheskiie osobennosti mikrominiaturizatsii polyprovodnikovykh okhlazhdaiushchikh termoelementov [Physical features of microminiaturization of semiconductor cooling thermoelements]. Candidate's thesis (Tech.sciences). Chernivtsi [in Russian].
28. Bartkowiak M., Mahan G.D. (2001). Heat and electricity transport through interfaces, in: *Recent Trends in Thermoelectric Materials, vol. II, Semiconductors and Semimetals*, vol. 70. New York: Academic Press.
29. Sze S.M. (1985). *Semiconductor Devices - Physics and Technology*, John Wiley & Sons.
30. Goldberg Yu.A. (1994). Ohmic contact metal-semiconductor AIIIBV: creation methods and properties. *Semiconductors*, 28(10), 1681-1698.
31. Da Silva L.W., Kaviany M. (2004). Microthermoelectric cooler: interfacial effects on thermal and electrical transport. *International Journal of Heat and Mass Transfer*, 47(10-11), 2417–2435.
32. Anatychuk L.I., Dugaev V.K., Litvinov V.I., Volkov V.L. (1994). Contact resistance between metal and thermoelectric material. *J. Thermoelectricity*, 1, 70-77.
33. Goltsman B.M., Kudinov I.A., Smirnov I.A. (1972). *Poluprovodnikovyie termoelektricheskiie materaily na osnove Bi_2Te_3 [Semiconductor thermoelectric materials based on Bi_2Te_3]*. Moscow: Nauka [in Russian].
34. Lifshits E.M., Pitaevskii L.P. (1979). *Fizicheskaia kinetika [Physical kinetics]*. Moscow: Nauka [in Russian].

Submitted 17.04.2019

V.V. Lysko, *cand. phys.– math. Sciences*[1,2]
Tudoroi P.F.[1,2]

[1]Institute of Thermoelectricity of the NAS and MES of Ukraine,
1, Nauky str, Chernivtsi, 58029, Ukraine;
e-mail: anatych@gmail.com
[2]Yu.Fedkovych Chernivtsi National University,
2, Kotsiubynskyi str., Chernivtsi, 58000, Ukraine

COMPUTER SIMULATION OF EXTRUSION PROCESS OF Bi_2Te_3 BASED TAPE THERMOELECTRIC MATERIALS

As long as in the process of hot extrusion of thermoelectric materials in the form of tape structures, billets of material are deformed under practically perfect plastic conditions, when optimizing equipment to obtain such materials, viscous fluid approximation may be used. This allows a computer simulation of the extrusion process using the hydrodynamic theory, where material is regarded as a fluid with a very high viscosity, which is a function of velocity and temperature. This paper presents the results of an object-oriented computer simulation of the process of hot extrusion of Bi_2Te_3 based thermoelectric material. Cases of producing thermoelectric materials in the form of tape structures for various matrix configurations are considered. The distributions of temperature and flow velocity of material in the matrix are obtained, as well as material velocity fields at the exit from the matrix which directly affect the structure of resulting material and its thermoelectric properties. Bibl. 6, Fig. 5, Tabl. 1.
Key words: simulationo, extrusion, tape thermoelectric material.

Introduction

At present, alongside with single-crystal *Bi-Te* based thermoelectric materials, extruded materials are also used for the production of thermoelectric products. The main advantage of the extrusion method is associated with improved material strength. Moreover, their thermoelectric properties may remain at the level of properties obtained by crystallization from the melt.

Generally, extruded thermoelectric materials are made in the form of cylindrical samples up to 25-30 mm in diameter. The use of extruded thermoelectric materials in the form of tape structures for the production of standard modules can reduce their cost by significantly reducing material losses.

At the same time, when creating equipment for producing extruded materials in the form of tape structures, the design and optimization of its structure are necessary.

One of effective ways to study the effect of conditions for producing material on its structure is mathematical simulation of the extrusion process in combination with the experimental results of structural studies [4, 5].

The purpose of this work is to create a computer model of the hot extrusion process of Bi_2Te_3 based thermoelectric material to study the distributions of temperature and material flow velocity in a rectangular-shaped matrix, which can be the basis for optimization of equipment for producing extruded thermoelectric material.

Physical, mathematical and computer extrusion models

To build a computer model of the hot extrusion process of tape thermoelectric material, the viscous fluid approximation and the application package of object-oriented simulation Comsol Multiphysics were